

Dual Electron Transfer Pathways from 4,4'-Dimethoxybenzophenone Ketyl Radical in the Excited State to Parent Molecule in the Ground State

Masanori Sakamoto, Xichen Cai, Mamoru Fujitsuka, and Tetsuro Majima*

The Institute of Scientific and Industrial Research (SANKEN), Osaka University, Mihogaoka 8-1, Ibaraki, Osaka 567-0047, Japan

Received: May 26, 2005

Dual intermolecular electron transfer (ELT) pathways from 4,4'-dimethoxybenzophenone (**1**) ketyl radical (**1H•**) in the excited state [**1H•**(D₁)] to the ground-state 4,4'-dimethoxybenzophenone [**1**(S₀)] were found in 2-methyltetrahydrofuran (MTHF) by observing bis(4-methoxyphenyl)methanol cation (**1H**⁺) and 4,4'-dimethoxybenzophenone radical anion (**1•**⁻) during nanosecond–picosecond two-color two-laser flash photolysis. ELT pathway I involved the two-photon ionization of **1H•** following the injection of electron to the solvent. The solvated electron was quickly trapped by **1**(S₀) to produce **1•**⁻. ELT pathway II was a self-quenching-like ELT from **1H•**(D₁) to **1**(S₀) to give **1H**⁺ and **1•**⁻. From the fluorescence quenching of **1H•**(D₁), the ELT rate constant was determined to be $1.0 \times 10^{10} \text{ M}^{-1} \text{ s}^{-1}$, which is close to the diffusion-controlled rate constant of MTHF. The self-quenching-like ELT mechanism was discussed on the basis of Marcus' ELT theory.

Introduction

Photoinduced electron transfer (ELT), which plays an important role in a broad array of processes in physical, chemical, and biological fields, attracts much attention from scientists.^{1,2} Generally, the lowest singlet and triplet excited states participate in photoinduced ELT. ELT from doublet states is also possible.^{3,4} Since radicals generally show enhanced donor or acceptor ability compared with the parent molecules, radicals in the excited state are expected to show quite high donor or acceptor abilities. Thus, ELT from radicals in the excited state is an attractive subject.⁴ However, studies on ELT from the excited doublet state are limited.^{3,4}

The well-established example of ELT from the excited radical is ELT between excited diphenyl methyl radical and electron donors or acceptors.^{4a–d} ELT from arylmethyl and ketyl radicals in the excited states was also observed with a series of amine, naphthalene, and onium salts as donor or acceptor.^{4b,d–k} The driving force dependence of the reaction rate constant was investigated on ELT from excited (4-cyanophenyl)phenylmethyl and 1-cyanonaphthylmethyl radicals to a series of dienes.^{4d}

For benzophenone ketyl radical, Scaiano and co-workers⁵ reported that the photoionization of benzophenone ketyl radical by excitation with a 515-nm dye laser generated a solvated electron (e_{solv}^-), which was quickly trapped by the ground-state benzophenone to produce benzophenone radical anion.

In the present investigation, we found dual intermolecular electron transfer (ELT) pathways from 4,4'-dimethoxybenzophenone (**1**) ketyl radical (**1H•**) in the excited state [**1H•**(D₁)] to the ground-state molecule [**1**(S₀)] during nanosecond–picosecond two-color two-laser flash photolysis. ELT pathway I included the two-photon ionization of **1H•**, generating e_{solv}^- , which was quickly trapped by **1**(S₀) to produce **1•**⁻. ELT pathway II was a self-quenching-like ELT from **1H•**(D₁) to **1**(S₀) to give **1H**⁺ and **1•**⁻ in the presence of high concentrations of

1(S₀). ELT from a radical in the excited state to the ground-state parent molecule was found for the first time. The dramatic change in electron donor or acceptor ability between **1**(S₀) and **1H•** was confirmed.

Experimental Section

The two-color two-laser flash photolysis experiment was carried out with the third harmonic oscillation (355 nm) of a nanosecond Nd³⁺:YAG laser (Quantel, Brilliant; 5 ns full width at half-maximum, fwhm) as the first laser and the second harmonic oscillation (532 nm) of a picosecond Nd³⁺:YAG laser (Continuum, RGA69-10; 30 ps fwhm) as the second laser. The delay time of the two laser flashes was adjusted to 1 μs by four-channel digital delay/pulse generators (Stanford Research Systems, Model DG 535). The breakdown of Xe gas generated by the fundamental pulse of the picosecond Nd³⁺:YAG laser was used as a probe light. Transient absorption spectra and kinetic traces were measured on a streak camera (Hamamatsu Photonics C7700) equipped with a charge-coupled device (CCD) camera (Hamamatsu Photonics C4742-98) and were stored on a PC. To avoid stray light and pyrolysis of the sample by the probe light, suitable filters were employed. The samples were allowed to flow in a transparent rectangular quartz cell (1.0 × 0.5 × 2.0 cm). For the measurements of both fluorescence spectra and decay profiles, the streak camera was used as the detector.

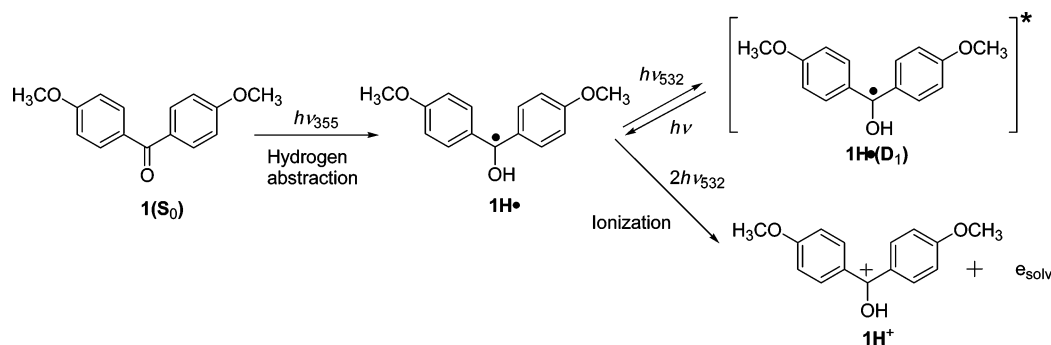
4,4'-Methoxybenzophenone was purchased from Tokyo Kasei and recrystallized three times from ethanol before use. Tetra-*n*-butylammonium azide was purchased from Tokyo Kasei and used as received. Sample solutions were prepared in 2-methyltetrahydrofuran (MTHF) and deoxygenated by bubbling with Ar gas for 30 min before irradiation. All experiments were carried out at room temperature.

Results and Discussion

Generation of Ketyl Radical in MTHF. **1H•** was generated by the photoreduction of **1** in MTHF. **1** in the triplet excited

* Corresponding author: e-mail majima@sanken.osaka-u.ac.jp.

SCHEME 1



state [$1(T_1)$] decayed through hydrogen abstraction from MTHF to produce $1H^\bullet$ after the first 355-nm nanosecond-laser irradiation (Scheme 1).⁶ The spectrum of $1H^\bullet$ with two peaks in the UV and visible regions agrees with the reported one (Figure 1).^{6a}

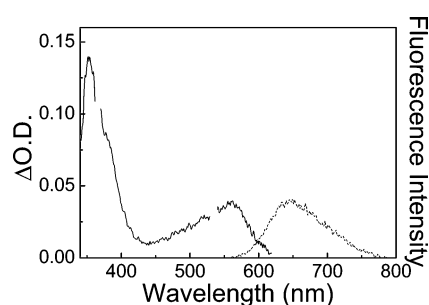


Figure 1. Absorption (solid line) and fluorescence (dotted line) spectra of $1H^\bullet$ in Ar-saturated MTHF at room temperature. The absorption spectrum was obtained during 355-nm laser flash photolysis, while the fluorescence spectrum was obtained during 355- and 532-nm two-color two-laser flash photolysis of 1 (5 mM). The discontinuity around 532 nm in the spectrum is due to residual SHG of the Nd³⁺:YAG laser.

Fluorescence Spectrum and Lifetime of 4,4'-Dimethoxybenzophenone Ketyl Radical in the Excited State. The generated $1H^\bullet$ was excited at the visible absorption band by use of the second laser (532 nm, 26 mJ pulse⁻¹, 30 ps fwhm) with a delay time of 1 μ s after the first laser (355 nm, 20 mJ pulse⁻¹, 5 ns fwhm). Upon excitation, $1H^\bullet$ showed fluorescence with a peak at 649 nm, which is almost a mirror image of the absorption spectrum of $1H^\bullet$ (Figure 1). The Stokes shift ($\Delta\nu_{ss}$) of $1H^\bullet$ was estimated to be 1.88×10^3 cm⁻¹. The energy gap between the D₁ and D₀ states of $1H^\bullet$ [$\Delta E(D_1 - D_0)$] was estimated to be 1.91 eV from the fluorescence maximum.

The fluorescence lifetime (τ_f) of $1H^\bullet$ was measured at the peak position of the fluorescence spectrum. The fluorescence decay curve was well fitted with the single-exponential decay function (Figure 2). The τ_f of $1H^\bullet$ was estimated to be 0.33 ± 0.02 ns when the concentration of $1(S_0)$ was 5 mM. The τ_f and fluorescence spectrum of $1H^\bullet$ in cyclohexane were similar to those in MTHF.⁷

ELT Pathway I: Solvated Electron Mediated ELT after the Two-Photon Ionization of 4,4'-Dimethoxybenzophenone Ketyl Radical. Immediately after the second laser irradiation, sharp and broad absorption bands appeared at 385 and 420–520 nm, respectively (Figure 3). The broad band centered at ca. 650 nm grew up within 1 ns. Since the lifetime of the broad band at 420–520 nm was 0.35 ns, which is essentially the same as the τ_f value, the broad band can be attributed to $1H^\bullet(D_1)$ (Figure 2). The broad band centered at ca. 650 nm (Figure 3), which has a long lifetime of 25 μ s, was assigned to be 4,4'-dimethoxybenzophenone radical anion ($1^{\bullet-}$).⁸ It is reported that

benzophenone ketyl radical was ionized upon excitation to inject electron into the solvent.⁵ The e_{solv}^- was quickly trapped by the ground-state benzophenone to produce the benzophenone radical anion.⁵ It is suggested that $1^{\bullet-}$ was generated from a similar stepwise reaction process (Scheme 2). The lifetime of the sharp band at 385 nm was 5.0 ns, which is quite different from those of $1H^\bullet(D_1)$ and $1^{\bullet-}$ (Figure 3). Therefore, it seems that the sharp band is another transient species. The bis(4-methoxyphenyl)methanol cation ($1H^+$) is a possible origin of the sharp band, as described in the next sections. Since $1H^+$ is expected to deprotonate quickly, producing $1(S_0)$, $1H^+$ would have a quite short lifetime compared with $1^{\bullet-}$ (Scheme 3).⁹ Although the same experiment was carried out for benzophenone ketyl radical, the sharp band was not observed during the 532-nm laser excitation of benzophenone ketyl radical. It is suggested that the diphenylmethanol cation would have absorption in a shorter wavelength region than $1H^+$ because the electron-donating substituents of $1H^+$ could stabilize the cation and cause a red shift of the absorption band.

A detailed investigation about the generation of $1H^+$ was carried out in acetonitrile. Since the hydrogen abstraction ability of $1(T_1)$ is negligible in acetonitrile, $1H^\bullet$ was generated by the bimolecular reaction of $1(T_1)$ with aniline. It is well-known that the benzophenone ketyl radical can be generated from the bimolecular reaction between amine and benzophenone(T_1).¹¹ The spectrum of $1H^\bullet$ in acetonitrile is shown in Figure 4 and shows good consistency with the reported one.^{6b} Following the second 532-nm excitation of $1H^\bullet$, fluorescence and an absorption band with a peak at 400 nm were generated (see Supporting Information Figures S1 and S2). The $\Delta\nu_{ss}$ of $1H^\bullet$ in acetonitrile was estimated to be 2.38×10^3 cm⁻¹. In our previous work, the $\Delta\nu_{ss}$ of $1H^\bullet$ in cyclohexane was estimated to be 1.68×10^3

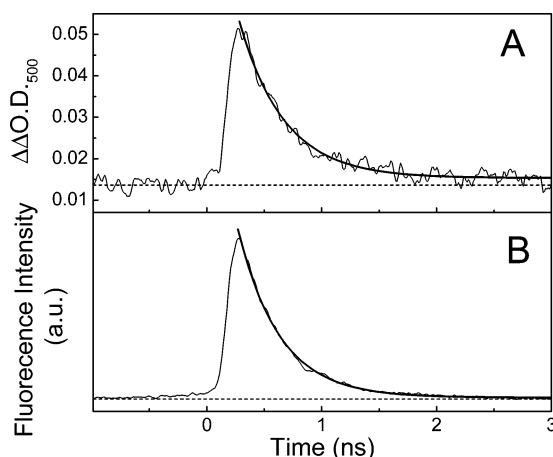


Figure 2. (A) Kinetic traces of $\Delta O.D.$ at 500 nm and (B) fluorescence intensity at 630 nm of $1H^\bullet$ during two-color two-laser photolysis. Solid lines are the best fits based on first-order kinetics.

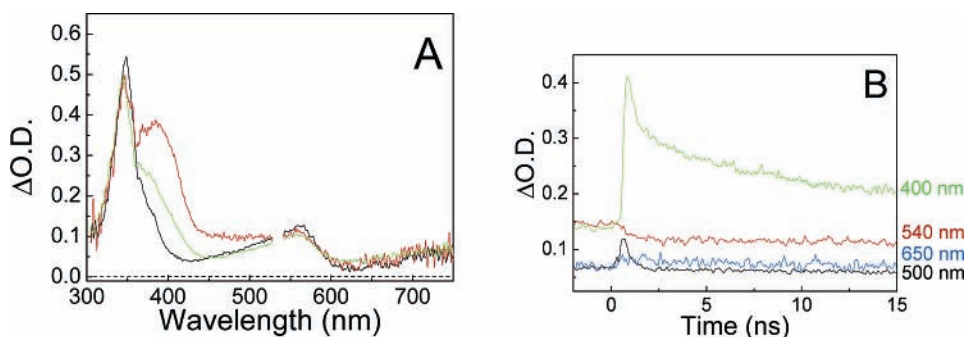
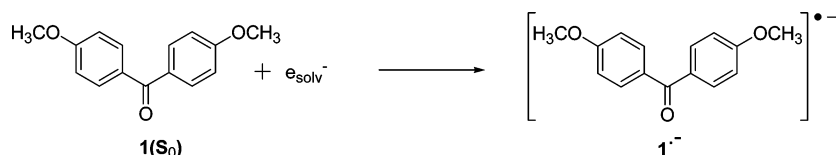
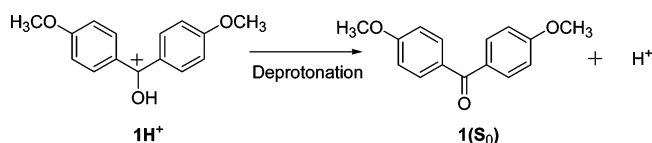


Figure 3. (A) Transient absorption spectra observed at 0.5 ns (red line) and 15 ns (green line) after the second laser irradiation during two-color two-laser photolysis (355 and 532 nm), and spectrum observed (black line) during one-laser photolysis (355 nm) of **1** (5 mM) in Ar-saturated MTHF. The second laser was employed 1 μ s after the first laser pulse. The discontinuity around 532 nm in the spectra is due to residual SHG of the Nd³⁺:YAG laser. (B) Kinetic traces of Δ OD at 400, 500, 540, and 650 nm (green, black, red, and blue lines, respectively) of **1H**[•] during two-color two-laser photolysis.

SCHEME 2



SCHEME 3



cm^{-1} .⁷ The dielectric constant of acetonitrile ($\epsilon = 35.94$)¹² was much larger than those of MTHF ($\epsilon = 6.97$)¹² and cyclohexane ($\epsilon = 2.023$).¹² The increase of $\Delta\nu_{\text{ss}}$ with increasing dielectric constant of solvent indicates the presence of dipole–dipole interaction between solvent and **1H**[•](D₁). It is noteworthy that the absorption band at 400 nm was red-shifted in acetonitrile, indicating that the transient species was also stabilized in polar media. The lifetime of the transient species was 11.3 ns, which is almost 2 times larger than that in MTHF. In the presence of tetra-*n*-butylammonium azide, a strong nucleophile,¹³ the ab-

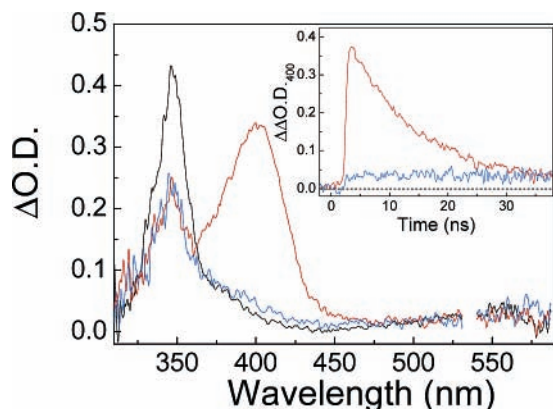


Figure 4. Transient absorption spectra observed 5 ns after the second laser irradiation during two-color two-laser photolysis (355 and 532 nm) with (blue line) and without (red line) *tert*-butylammonium azide (0.1 M), and spectrum observed (black line) during one-laser photolysis (355 nm) of **1** (5 mM) in Ar-saturated acetonitrile containing *N,N*-diethylaniline (0.055 M). The second laser was employed 1 μ s after the first laser pulse. The discontinuity around 532 nm in the spectra is due to residual SHG of the Nd³⁺:YAG laser. (Inset) Kinetic traces of Δ OD at 400 nm with (blue line) and without (red line) *tert*-butylammonium azide during two-color two-laser photolysis.

sorption band completely disappeared due to nucleophilic attack, supporting the hypothesis that the sharp absorption band at 400 nm was assigned to **1H**[•]. The component that did not disappear in the presence of tetra-*n*-butylammonium azide was assigned to be **1^{•-}**.⁸ It is noteworthy that **1H**[•] is difficult to generate from other methods. Two-color two-laser flash photolysis provides a useful method to generate **1H**[•].

To elucidate the mechanism of ionization of **1H**[•], the laser power (I in millijoules per pulse) dependence of the ionization yield was investigated (Figure 5). When ionization of **1H**[•] occurs through the two-photon process, the slope of plots of $\log \Delta\text{OD}_{385}$ versus $\log I$ will be around 2. Plots of $\log \Delta\text{OD}_{385}$ versus $\log I$ show the linear correlation with a slope of 2.0 at the laser fluence of 6–23 mJ pulse⁻¹ in MTHF, indicating that the formation of **1H**[•] is via the two-photon process. In acetonitrile, the plots of $\log \Delta\text{OD}_{400}$ versus $\log I$ also show linear correlation with a slope of 1.8. These results also support the identification of the absorption band at 385 nm in MTHF (400 nm in acetonitrile) as **1H**[•]. It is indicated that the ionization of **1H**[•] occurred through the two-photon process in both solvents. Thus, ionization potential of **1H**[•] was roughly estimated to be between $2.3 + E(\text{D}_0)$ and $4.6 + E(\text{D}_0)$ eV, taking the photon energy of 532 nm laser into account. $E(\text{D}_0)$ is an energy of **1H**[•] relative to **1(S₀)**. By employing the heat of formation ($\Delta H_f = 0.91$ eV) of benzophenone ketyl radical as the $E(\text{D}_0)$ value,¹⁴ the ionization potential of **1H**[•] is expected to be between 3.1 and 5.5 eV. To the best of our knowledge, there is no report about the photoinduced ionization of **1H**[•] in MTHF at room temperature.

From the above-mentioned results, it is concluded that **1H**[•] is generated by the stepwise reactions as shown in Schemes 1–2 after the second laser irradiation of **1H**[•]. First, a part of **1H**[•] was ionized upon the second laser excitation to generate **1H**⁺ and e_{solv}^- . Second, e_{solv}^- was trapped by **1(S₀)** to produce **1^{•-}** (Scheme 4).

ELT Pathway II: Intermolecular ELT from 4,4'-Dimethoxybenzophenone Ketyl Radical in the Excited State to Ground-State Parent Molecule. The two-color two-laser experiment on **1H**[•] was carried out in the presence of high concentrations of **1(S₀)** (0.02–0.1 M). It was revealed that the

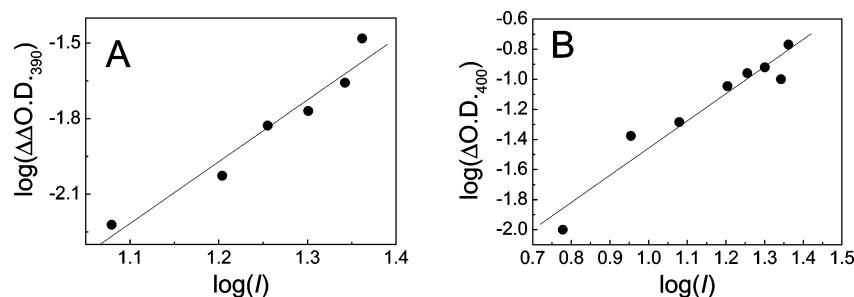
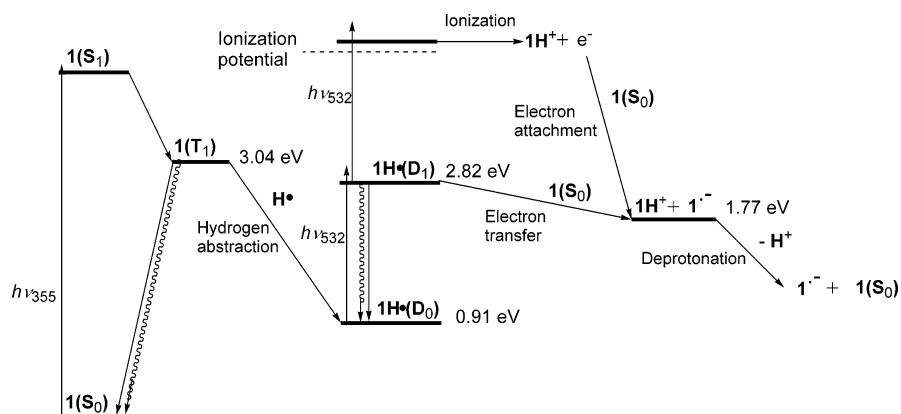


Figure 5. Plots of $\log \Delta\Delta OD$ vs $\log I$ in (A) MTHF and (B) acetonitrile. The I values are in millijoules per pulse.

SCHEME 4



fluorescence intensity of $1H^{\bullet}(D_1)$ decreased with increasing concentrations of $1(S_0)$. The decrease of fluorescence intensity of $1H^{\bullet}(D_1)$ indicates the presence of a reaction pathway between $1H^{\bullet}(D_1)$ and $1(S_0)$. Three reaction pathways were possible: (i) ELT from $1H^{\bullet}(D_1)$ to $1(S_0)$, (ii) proton transfer from $1H^{\bullet}(D_1)$ to $1(S_0)$, and (iii) another chemical reaction between $1H^{\bullet}(D_1)$ with $1(S_0)$, such as the cross-linking reaction reported for xanthone ketyl radical in the excited state and xanthone in the ground state.¹⁵ Since the generation of $1H^{\bullet}(D_0)$ was not observed after the second laser irradiation, possibility ii can be eliminated. According to the result of product analysis following the excitation of benzophenone ketyl radical by two-color two laser flash photolysis, no product that derived from the reaction between $1H^{\bullet}(D_1)$ and $1(S_0)$ was reported.¹⁵ Thus, possibility iii was also negligible. To clarify the reaction pathway i, we measured the generation rate of $1^{\bullet-}$ under a high concentration of $1(S_0)$ (0.05 M). When $1^{\bullet-}$ was generated from the bimolecular reaction from $1H^{\bullet}(D_1)$, the decay rate of $1H^{\bullet}(D_1)$ and generation rate of $1^{\bullet-}$ should be the same. The generation rate of $1^{\bullet-}$ was estimated to be $(3.1 \pm 0.8) \times 10^9 \text{ s}^{-1}$, which agrees with the decay rate constant of $1H^{\bullet}(D_1)$ ($2.9 \times 10^9 \text{ s}^{-1}$) (Figure 6). Therefore, it can be concluded that $1H^+$ and $1^{\bullet-}$ were

generated by intermolecular ELT from $1H^{\bullet}(D_1)$ to $1(S_0)$ in the presence of high concentrations of $1(S_0)$ (Scheme 5).

Rate Constant of ELT from 4,4'-Dimethoxybenzophenone Ketyl Radical in the Excited State. To determine the fluorescence quenching rate, τ_f was measured as a function of the concentration of $1(S_0)$. The reaction process between $1H^{\bullet}(D_1)$ and $1(S_0)$ leads to a shorter τ_f value of $1H^{\bullet}(D_1)$ with increasing concentration of $1(S_0)$. From the plot of $1/\tau_f$ against $[1(S_0)]$ (Figure 7), the ELT quenching rate constant (k_{ELT}) was determined according to¹⁶

$$\frac{1}{\tau_f} = \frac{1}{\tau_{f0}} + k_{\text{ELT}}[1(S_0)] \quad (1)$$

where τ_{f0} denotes the intrinsic fluorescence lifetime, which was estimated from the intercept of the plot of Figure 7 to be $0.36 \pm 0.2 \text{ ns}$. The k_{ELT} value of $1H^{\bullet}(D_1)$ was estimated to be $1.0 \times 10^{10} \text{ M}^{-1} \text{ s}^{-1}$, which is similar to the diffusion-controlled rate constant of MTHF ($1.2 \times 10^{10} \text{ M}^{-1} \text{ s}^{-1}$).¹⁷

We examined to estimate the ELT rate by use of Marcus' ELT theory.¹⁸ The ELT rate depends on the driving force ($-\Delta G_{\text{ELT}}$). $-\Delta G_{\text{ELT}}$ of the ELT from $1H^{\bullet}(D_1)$ to $1(S_0)$ is represented by^{4j,18}

$$\Delta G_{\text{ELT}} = E_{\text{ox}} - E_{\text{red}} + w_p + e^2 \left(\frac{1}{2r_1} + \frac{1}{2r_2} \right) \left(\frac{1}{\epsilon_s} - \frac{1}{\epsilon_{\text{sp}}} \right) - \Delta E(D_1 - D_0) \quad (2)$$

where E_{ox} is the oxidation potential of $1H^{\bullet}$, E_{red} is the reduction potential of 1 (-2.02 V vs SCE in acetonitrile),¹⁰ w_p is Coulombic energy (-0.3 eV),¹⁹ e is electronic charge, r_1 and r_2 are ionic radii ($\sim 7 \text{ \AA}$), ϵ_s is the dielectric constant of MTHF, and ϵ_{sp} is the dielectric constant of acetonitrile. With the assumption that E_{ox} of $1H^{\bullet}$ is similar to that of benzophenone ketyl radical ($E_{\text{ox}} = -0.25 \text{ V}$ vs SCE in acetonitrile),²⁰ the $-\Delta G_{\text{ELT}}$ value was estimated to be 0.16 eV (Scheme 4).

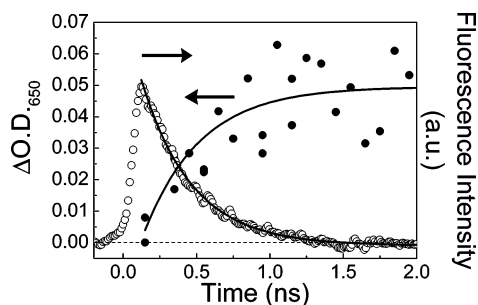
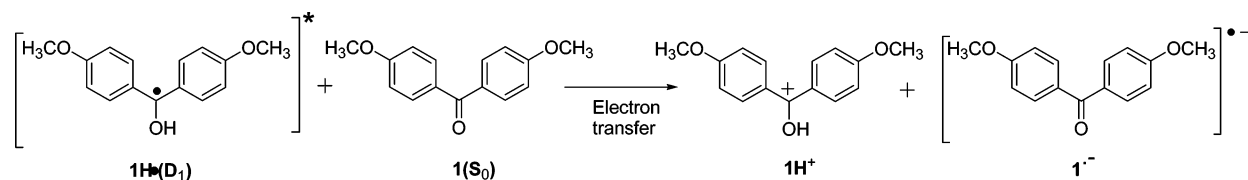


Figure 6. Kinetic traces of ΔOD at 650 nm (\bullet) and fluorescence intensity (\circ) of $1H^{\bullet}$ during two-color two-laser photolysis.

SCHEME 5



According to Marcus' ELT theory, the activation energy (ΔG^*) can be simply represented by^{1,2}

$$\Delta G^* = \frac{\lambda_s}{4} \left(1 + \frac{\Delta G}{\lambda_s} \right)^2 \quad (3)$$

where λ_s is an intrinsic barrier corresponding to the solvent reorganization mainly. The solvent reorganization energy (λ_s) of MTHF was reported to be 0.86 eV.²¹ In simplified form, the activation-energy-controlled ELT rate constant can be expressed by

$$k_{\text{ELT}} = \nu \exp\left(\frac{-\Delta G^*}{RT}\right) \quad (4)$$

where ν is the frequency factor. Here, ν is assumed to be $1.0 \times 10^{13} \text{ M}^{-1} \text{ s}^{-1}$.^{2b} From eqs 3 and 4, k_{ELT} was estimated to be $3.5 \times 10^{10} \text{ M}^{-1} \text{ s}^{-1}$. For the bimolecular reaction, when the formation of an encounter complex is taken into account,² the electron-transfer rate constant (k_{ELT}') can be given by

$$\frac{1}{k_{\text{ELT}}'} = \frac{1}{k_{\text{diff}}} + \frac{1}{k_{\text{ELT}}} \quad (5)$$

where k_{diff} is the diffusion-controlled rate constant. From eq 5, k_{ELT}' was estimated to be $1.2 \times 10^{10} \text{ M}^{-1} \text{ s}^{-1}$, which is similar to the ELT rate constant estimated by the Stern–Volmer treatment.

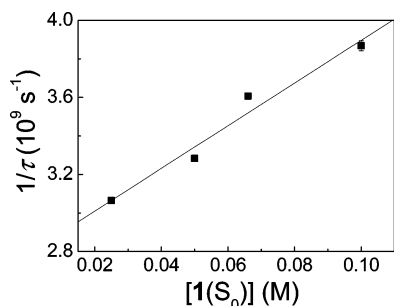


Figure 7. Plots of $1/\tau$ vs $[1(S_0)]$.

In nonpolar solvents such as MTHF, the charge recombination process should play an important role in an efficient intermolecular ELT process due to the slow dissociation rate of products. It is supposed that the intermolecular ELT from $1\text{H}^+(\text{D}_1)$ to $1(\text{S}_0)$ was observed due to the inefficient charge recombination process.

Conclusions

In the present study, we found the dual electron-transfer pathways of $1\text{H}^+(\text{D}_1)$ to $1\text{H}^+(\text{S}_0)$ in MTHF (Scheme 4) using two-color two-laser flash photolysis. ELT pathway I involved the two-photon ionization of 1H^+ following the injection of electron to the solvent. e_{solv}^- was quickly trapped by $1(\text{S}_0)$ to produce $1^{\bullet-}$. ELT pathway II was the self-quenching-like ELT from $1\text{H}^+(\text{D}_1)$ to $1(\text{S}_0)$ to give 1H^+ and $1^{\bullet-}$. From the fluorescence quenching of $1\text{H}^+(\text{D}_1)$, the ELT rate constant was

determined to be $1.0 \times 10^{10} \text{ s}^{-1}$, which agreed well with the value estimated by Marcus' ELT theory. The absorption spectrum originating from the unique cation of 1H^+ was detected for the first time. The self-quenching-like ELT mechanism was discussed on the basis of energetic considerations. The recombination process would play important roles in intermolecular ELT from the doublet excited state.

Acknowledgment. This work has been partly supported by a Grant-in-Aid for Scientific Research [Project 17105005, Priority Area (417), 21st Century COE Research, and others] from the Ministry of Education, Culture, Sports, Science and Technology (MEXT) of the Japanese Government.

Supporting Information Available: Transient absorption following the second 532-nm laser excitation of 1H^+ , kinetic traces of $1\text{H}^+(\text{D}_1)$, and fluorescence of 1H^+ in acetonitrile. This material is available free of charge via the Internet at <http://pubs.acs.org>.

References and Notes

- (1) Balzani, V. *Electron Transfer in Chemistry*, Vols. 1–5; Wiley–VCH: Weinheim, Germany, 2001–2002.
- (2) (a) Marcus, R. A.; Sutin, N. *Biochim. Biophys. Acta* **1985**, *811*, 265. (b) Kavarnos, G. J.; Turro, N. *J. Chem. Rev.* **1986**, *86*, 401. (c) Gould, I. R.; Ege, D.; Moser, J. E.; Farid, S. *J. Am. Chem. Soc.* **1990**, *112*, 4290.
- (3) (a) Ramamurthy, V.; Schanze, K. S. *Molecular and supramolecular photochemistry*, Vol. 2; Marcel Dekker: New York, 1994. (b) Scaiano, J. C.; Johnston, L. J.; McGimpsey, W. G.; Weir, D. *Acc. Chem. Res.* **1988**, *21*, 22. (c) Melnikov, M. Y.; Smirnov, V. A. *Handbook of Photochemistry of Organic Radicals*; Begell House: New York, 1996.
- (4) (a) Arnold, B. R.; Scaiano, J. C.; McGimpsey, W. G. *J. Am. Chem. Soc.* **1992**, *114*, 9978. (b) Scaiano, J. C.; Tanner, M.; Weir, D. *J. Am. Chem. Soc.* **1985**, *107*, 4396. (c) Johnston, L. J.; Scaiano, J. C. *J. Am. Chem. Soc.* **1985**, *107*, 6368. (d) Weir, D. *J. Phys. Chem.* **1990**, *94*, 5870. (e) Weir, D.; Johnston, L. J.; Scaiano, J. C. *J. Phys. Chem.* **1988**, *92*, 1742. (f) Fox, M. A.; Gaillard, E.; Chen, C.-C. *J. Am. Chem. Soc.* **1987**, *109*, 7088. (g) Netto-Ferreira, J. C.; Scaiano, J. C. *J. Chem. Soc., Chem. Commun.* **1989**, 435. (h) Adam, W.; Oestrich, R. S. *J. Am. Chem. Soc.* **1992**, *114*, 6031. (i) Johnston, L. J.; Lougnot, D. J.; Wintgens, V.; Scaiano, J. C. *J. Am. Chem. Soc.* **1988**, *110*, 518. (j) Baumann, H.; Merckel, C.; Timpe, H.-J.; Graness, A.; Kleinschmidt, J.; Gould, I. R.; Turro, N. *J. Chem. Phys. Lett.* **1984**, *103*, 497. (k) Samanta, A.; Bhattacharyya, K.; Das, P. K.; Kamat, P. V.; Weir, D.; Hug, G. L. *J. Phys. Chem.* **1989**, *93*, 3651.
- (5) (1) Redmond, R. W.; Scaiano, J. C.; Johnston, L. J. *J. Am. Chem. Soc.* **1990**, *112*, 398. (2) Redmond, R. W.; Scaiano, J. C.; Johnston, L. J. *J. Am. Chem. Soc.* **1992**, *114*, 9768.
- (6) (a) Baral-Tosh, S.; Chattopadhyay, S. K.; Das, P. K. *J. Phys. Chem.* **1984**, *88*, 1404. (b) Bhattacharyya, K.; Das, P. K. *J. Phys. Chem.* **1986**, *90*, 3987. (c) Akiyama, K.; Sekiguchi, S.; Tero-Kubota, S. *J. Phys. Chem.* **1996**, *100*, 180. (d) Bhasikuttan, A. C.; Singh, A. K.; Palit, D. K.; Sapre, A. V.; Mittal, J. P. *J. Phys. Chem. A* **1998**, *102*, 3470. (e) Bergamini, G.; Ceroni, P.; Maestri, M.; Balzani, V.; Lee, S.-K.; Vögtle, F. *Photochem. Photobiol. Sci.* **2004**, *3*, 898. (f) Hoffman, M.; Görner, H. *Chem. Phys. Lett.* **2004**, *383*, 451.
- (7) Sakamoto, M.; Cai, X.; Hara, M.; Tojo, S.; Fujitsuka, M.; Majima, T. *J. Phys. Chem. A* **2004**, *108*, 8147.
- (8) *Electronic absorption spectra of radical ions*; Physical Science Data 34; Shida, T., Ed.; Elsevier: Amsterdam, 1988.
- (9) (a) Bietti, M.; Lanzalunga, O. *J. Org. Chem.* **2002**, *67*, 2632. (b) Bacciochi, E.; Bietti, M.; Steenken, S. *Chem. Eur. J.* **1999**, *5*, 1785. (c) Bacciochi, E.; Belvedere, S.; Bietti, M.; Lanzalunga, O. *Eur. J. Org. Chem.* **1998**, *3*, 299.
- (10) *Handbook of Photochemistry*, 2nd ed; Murov, S. L., Carmichael, I., Hug, G. L., Eds.; Marcel Dekker: New York, 1993.

- (11) (a) Matsushita, Y.; Kajii, Y.; Obi, K. *J. Phys. Chem.* **1992**, *96*, 4455. (b) Arimitsu, S.; Masuhara, H.; Mataga, N.; Tsubomura, H. *J. Phys. Chem.* **1975**, *79*, 1255. (c) Simon, J. D.; Peters, K. S. *J. Am. Chem. Soc.* **1983**, *105*, 4875. (d) Miyasaka, H.; Morita, K.; Kamada, K.; Mataga, N. *Chem. Phys. Lett.* **1991**, *178*, 504. (e) Miyasaka, H.; Morita, K.; Kamada, K.; Nagata, T.; Kiri, M.; Mataga, N. *Bull. Chem. Soc. Jpn.* **1991**, *64*, 3229. (f) Peters, K. S.; Kim, G. *J. Phys. Chem. A* **2004**, *108*, 2598.
- (12) *Techniques of chemistry*, Vol. 2, 4th ed.; Riddick, J. A., Bunger, W. B., Sakano, T. K., Eds.; John Wiley and Sons: New York, 1986.
- (13) (a) Johnston, L. J.; Lobaugh, J.; Wintgens, V. *J. Phys. Chem.* **1989**, *93*, 7370. (b) Alonso, E. O.; Johnston, L. J.; Scaiano, J. C.; Toscano, V. G. *J. Am. Chem. Soc.* **1990**, *112*, 1270. (c) McClelland, R. A.; Kanagasabapathy, V. M.; Banait, N. S.; Steenken, S. *J. Am. Chem. Soc.* **1991**, *113*, 1009. (d) Faria, J. L.; Steenken, S. *J. Phys. Chem.* **1992**, *96*, 10869. (e) Davids, P. A.; Kahley, M. J.; McClelland, R. A.; Novak, M. *J. Am. Chem. Soc.* **1994**, *116*, 4513. (f) Pohlers, G.; Scaiano, J. C.; Step, E.; Sinta, R. *J. Am. Chem. Soc.* **1999**, *121*, 6167. (g) Shukla, D.; Lu, C.; Schepp, N. P.; Bentrude, W. G.; Johnston, L. J. *J. Org. Chem.* **2000**, *65*, 6167.
- (14) (a) Takeda, K.; Kajii, Y.; Shibuya, K.; Obi, K. *J. Photochem. Photobiol., A* **1998**, *115*, 109. (b) Arnaut, L. G.; Caldwell, R. A. *J. Photochem. Photobiol., A* **1992**, *65*, 15.
- (15) (a) Adam, W.; Kita, F.; Oestrich, R. F. *J. Photochem. Photobiol., A* **1994**, *80*, 187. (b) Adam, W.; Kita, F. *J. Am. Chem. Soc.* **1994**, *116*, 3680.
- (16) *Modern Molecular Photochemistry*; Turro, N. J., Ed.; Benjamin/Cummings Publishing Co.: Menlo Park, CA, 1978.
- (17) Sakamoto, M.; Cai, X.; Hara, M.; Tojo, S.; Fujitsuka, M.; Majima, T. *J. Phys. Chem. A* **2005**, *109*, 2452.
- (18) Weller, A. *Z. Phys. Chem. Neue Folge* **1982**, *133*, 93.
- (19) w_p was given by $w_p = e^2/d\epsilon_s$, where e is electric charge, d is the distance between donor and acceptor, and ϵ_s is a dielectric constant of MTHF. We employed the values $d = 7 \text{ \AA}$ and $\epsilon_s = 6.97$.¹²
- (20) Lund, T.; Wayner, D. D. M.; Jonsson, M.; Larsen, A. G.; Daasbjerg, K. *J. Am. Chem. Soc.* **2001**, *123*, 12590.
- (21) Hayes, R. T.; Walsh, C. J.; Wasielewski, M. R. *J. Phys. Chem. A* **2004**, *108*, 2375.